Recombination of an atomic system in one, two, and three dimensions in the presence of an ultrastrong attosecond laser pulse: A comparison of results obtained using a Coulomb and a smoothed Coulomb potential

Tomasz Dziubak and Jacek Matulewski*
Instytut Fizyki, Uniwersytet Mikołaja Kopernika, ul. Grudziadzka 5, 87-100 Toruń, Poland
(Received 18 February 2008; revised manuscript received 30 December 2008; published 1 April 2009)

The dynamics of recombination in an ultrastrong laser field is studied by numerical simulations performed for one-dimensional (1D), two-dimensional, and three-dimensional atomic systems modeled by the hydrogen atom Coulomb potential as well as by a model potential with a smoothed core. A nonmonotonic behavior of the total bound-states' final population is studied as a function of the laser field amplitude. The dependence of the results on the used atomic potential is demonstrated. It is shown that the recombination probabilities calculated in these two cases may differ even qualitatively. Even eigenstates of the 1D hydrogen atom are shown to play a significant role in the time evolution.

DOI: 10.1103/PhysRevA.79.043404 PACS number(s): 34.50.Rk, 32.80.Wr, 34.80.Lx

I. INTRODUCTION

The interest in attosecond (few-cycle) pulses is motivated by recent experimental realizations of such pulses by groups from Germany and Canada [1]. Attosecond pulses of extreme-ultraviolet or soft x-ray laserlike sources have already been found very useful for investigating details of an evolution of biological, chemical, and even atomic systems [2]. Using so short pulses, one may create a sort of movie presenting an evolution of a molecule. Attosecond laser technology is very new; thus new ideas of its applications continue to appear, including those in material science such as, e.g., identifying elements, precise cutting of materials not resistant to heat, and others [3]—however there is still a long way to a practical realization.

An interaction of an ultrastrong laser field with atomic systems is accompanied by a characteristic phenomenon called adiabatic stabilization against photoionization; the ionization probability is locally a decreasing function of the field intensity [4,5]. This counterintuitive feature of strong-field ionization occurs for laser fields intensity of a few atomic units (a.u.) if the laser cycle frequency is about unity. This phenomenon is usually explained in terms of the Kramers-Henneberger (KH) well [5], which is the mean potential (zeroth term of the Fourier expansion) of the oscillating nucleus in the electron reference frame. One should also take into account the influence of the so-called slow drift, i.e., long-time oscillations caused by an interaction of an oscillating electron driven by the field with the original potential. It can be incorporated to the KH well theory [6] and may be decisive for the value of the ionization level [6–8].

In our previous papers we have found a very similar effect of a nonmonotonic dependence of the total bound-states' population on the electric field of an ultrastrong attosecond laser pulse in the case of a recombination in the presence of a one-dimensional (1D) short-range potential (square well) [9] as well as of the 1D long-range potential [10]. However, in the latter case only a model atom with a smoothed potential was investigated and only the ground-state population was taken into account. We have also examined the same quantity in the two-dimensional (2D) square well but no nonmonotonic behavior has been found in that case [9]. In all the above cases the discussed phenomenon was attributed mainly to the slow drift of the wave packet trapped in the KH well. Some aspects of the strong-field recombination were earlier examined by Hu and Collins [11], who concentrated on the dependence of the process on the initial momentum of the incoming electron.

Up to now the ultrastrong laser-assisted recombination has been studied in one dimension for both short- and long-range binding potentials [10] and in two dimensions for short-range ones [9]. In the present paper we examine the cases of two- and three-dimensional (3D) systems with long-range potentials. In particular we compare the results for two- and three-dimensional Coulomb singular and smoothed binding potentials, and we observe substantial differences (Secs. III A and III B). Because of those differences and the fact that a smoothed Coulomb potential has been widely used in numerical studies, we return to the one-dimensional case (Sec. III C) in order to check whether the models with such potentials are reliable in the studies of recombination. Here we compare the results for the two classes of long-range potentials. We have also improved our approach by taking into account all the significant bound states when calculating the recombination level. For the unsmoothed potential in one dimension a degeneracy of even and odd states occurs. Because the wave function of the former ones is nondifferentiable at the origin, their physical status has been questioned [12–14]. We thus examine the role of such states in the context of laser-assisted recombination.

II. NUMERICAL APPROACH

A. Hamiltonian of the atom-laser system

A three-dimensional atomic system in a strong laser field may be described using the Hamiltonian in the length gauge (a.u. are used throughout the paper),

*jacek@phys.uni.torun.pl

$$\hat{H} = -\frac{1}{2}\left(\frac{\partial^2}{\partial x^2} + \frac{\partial^2}{\partial y^2} + \frac{\partial^2}{\partial z^2}\right) + V(\sqrt{x^2+y^2+z^2}) + z\varepsilon(t), \tag{1}$$

where the laser electric field $\varepsilon(t)=\varepsilon_0\Theta(t)\Theta(t_f-t)\cos(\omega t-\pi)$ is directed along the z axis and due to the dipole approximation does not depend on the spatial coordinates (Θ denotes here the Heaviside function). It acts only during the time interval $(0,t_f)$. In all our calculations the laser field frequency ω has been taken equal to 1 a.u. and the optical period is equal to $T=2\pi$ a.u. We have changed the laser field amplitude ε_0 in the range between 1 and 5 a.u. in two and three dimensions and between 1 and 7 a.u. in one dimension.

The dipole approximation used in all the calculations presented below is known to be fully justified even for laser fields of order of a few a.u. [15] while our strongest field was $\varepsilon_0=7$ a.u. Also in our earlier paper we checked that for the laser frequency $\omega=1$ a.u. in two dimensions, the nondipole (magnetic) effects begin to be important for fields of order of $\varepsilon_0\approx 15$ a.u. [7,8].

The class of long-range binding potential we studied is given by

$$V(\sqrt{x^2+y^2+z^2}) = V(r) = -\frac{1}{\sqrt{a^2+r^2}}, \tag{2}$$

where $r=\sqrt{x^2+y^2+z^2}$. For $a=0$ a.u. this is the standard singular hydrogen atom potential and for $a=1$ a.u.—a model atom with a smoothed core, which in the case of one dimension ($y=z=0$) reduces to the model proposed first by Su and Eberly [16]. We have been mainly concerned with these two limiting cases.

As the initial state of the electron we used a Gauss function of a fully symmetric shape, located on the z axis at some distance from the nucleus (see also the discussion below). Due to the linear polarization and the dipole approximation our 3D system possesses an axial symmetry; thus it is useful to apply cylindrical coordinates $\{s,\varphi,z\}$. This allows one to separate the angular function $\exp(im\varphi)$. For the sake of convenience we have also made a substitution for the spatial part of the wave function (dependent on s and z) $\tilde{\Psi}=\Psi/\sqrt{s}$ so that the first derivative of the Laplace operator in the cylindrical coordinates is removed. Instead, an additional potential-like term $-1/(8s^2)$ appears which may be incorporated to the sort of effective potential (cf. [17] for its more extensive discussion). Thus we obtain the following Schrödinger equation to be solved numerically:

$$i\frac{\partial}{\partial t}\tilde{\Psi}(s,z,t) = -\frac{1}{2}\left(\frac{\partial^2}{\partial s^2} + \frac{\partial^2}{\partial z^2}\right)\tilde{\Psi}(s,z,t) + \left[V(\sqrt{s^2+z^2}) + \frac{1}{2}\frac{m^2-1/4}{s^2} + z\varepsilon(t)\right]\tilde{\Psi}(s,z,t). \tag{3}$$

The quantum number m is connected with the rotation around the z axis and is constant during the whole process. For $m=0$ the potential-like term is attractive. A nonzero value of m makes it repulsive, and as a consequence it completely modifies the wave-packet dynamics, the simulation of which must be performed separately for each m. Since the value of m is conserved during the whole evolution, in the case of the initial state given by a Gauss function with $m=0$ only the states with $m=0$ may be populated, including the most interesting ground state. This makes the assumption of $m=0$ a natural choice for investigating the recombination process.

The boundary condition for $\tilde{\Psi}$ at $s=0$ is such that the value of the wave function $\tilde{\Psi}$, and not its derivative, should vanish. An additional benefit of using $\tilde{\Psi}$ instead of Ψ is that the Jacobian becomes equal to 1; thus three-dimensional simulations may be performed using the same code as that prepared for 2D calculation in Cartesian coordinates with only minimal changes, namely, the modification of the potential to include the new term.

As a consequence only two-dimensional numerical calculations have to be performed in the $\{s,z\}$ coordinates to obtain accurate results for a three-dimensional system with a linearly polarized external field. We also performed analogous simulations in one and two dimensions. To keep the z direction of the electric field we use the $\{x,z\}$ Cartesian coordinates for the two-dimensional system and $\{z\}$ for the one-dimensional one. Thus the Hamiltonian of the 2D atom interacting with the laser field may be written as

$$\hat{H} = -\frac{1}{2}\left(\frac{\partial^2}{\partial x^2} + \frac{\partial^2}{\partial z^2}\right) + V(\sqrt{x^2+z^2}) + z\varepsilon(t). \tag{4}$$

The one-dimensional form of the Hamiltonian may be obtained by setting $x=0$. The axial symmetry of the 3D system has its counterpart in the 2D case—if the initial state is given by symmetric function one can perform the calculation only at the half of the x-z plane, i.e., for $x>0$.

B. Initial conditions

During the recombination an initially remote packet arrives in the vicinity of the nucleus; its motion is in general a superposition of translation and oscillations in the rhythm of the external laser field. A considerable capture probability may occur if the pulse has such a shape that the corresponding electron classical trajectory remains in the neighborhood of the nucleus and the initial conditions are such that the electron turning point occurs in the vicinity of the nucleus. Thus to shorten the numerical calculations we start our simulations at the moment at which the electron is located at the distance from the nucleus equal to twice the amplitude of its free oscillations, and we assume that its initial momentum is zero (the dependence of the recombination level on the initial momentum in the 2D case has already been examined in [11]). These conditions favor the situation in which the electron wave packet after a half of an optical cycle will be situated close to the center of the binding potential with a small momentum (very close to the turning point of its oscillatory motion). Unfortunately, by setting the initial wave packet relatively close to the nucleus we increase the initial occupation of higher excited states (see the discussion below). Moreover, the wave packet should be still relatively narrow. Other electrons from a beam, i.e., those which have

different positions and velocities after a half of an optical cycle, have fewer chances to recombine with the ion. The same approach in the case of the electron incoming in fact from infinity was applied in [9,10]. The sensibility of the results to the packet initial position was also checked in [10], including an examination whether the results remain valid if an average over the initial position is taken. This will also be checked in the present paper for attosecond pulses.

Because of the above, in our simulations the initial position of the electron modeled by a Gaussian packet was adjusted to the electric field intensity ε_0 applied in a given simulation and equal to $z_0=-2\varepsilon_0/\omega^2$. Thus the initial state of the electron is given by the following wave function:

$$\psi(x,y,z) = C\exp\{-[x^2+y^2+(z-z_0)^2]/(4\delta^2)\}, \qquad (5)$$

with C being the normalization constant.

The variance of the wave packet is fixed at $\delta^2=0.25$ a.u. in all 3D, 2D, as well as in 1D simulations. In the 3D case in the reduced cylindrical coordinates the above function behaves (up to the normalization constant) as

$$\psi(s,\varphi,z) \sim \exp\{-[s^2+(z-z_0)^2]/(4\delta^2)\}, \qquad (6)$$

note that the value of the quantum number m for this packet is equal to 0.

C. Determination of the bound states

Unlike in our previous study of the 1D recombination of an electron with an ion described by a long-range potential [10], we take now into account the presence of the excited states and examine their populations. We also extend our investigations to the two- and three-dimensional cases, and what is most important, we now investigate the dependence of the results on the precise shape of the potential. The eigenstates in the case of the one-, two-, and three-dimensional singular Coulomb potentials may be found analytically (for 1D hydrogen atom see [12–14]), for a discussion on the 2D hydrogen atom see [18]). In one and two dimensions the wave function is given by a confluent hypergeometric function of the first kind ${}_1F_1$ (Kummer's function); however the one-dimensional case is still not clearly understood. Namely, the discussion continues whether the states with even symmetry have any physical meaning. Loudon [12] claimed that only by taking the eigenstates with both parities one may create a complete basis in the Hilbert space, while Palma and Raff [14] as well as Dai *et al.* [13] held the opinion that even states are not physical because of a discontinuity of the derivative of their wave functions at the point of the potential singularity. We checked in our simulations the population of the eigenstates with both even and odd parities. It seems that both classes of states are significantly occupied by the recombining electron. The energy of eigenstates of the two-dimensional singular hydrogen atom depends only on the main quantum number N and is equal to $E_N=-1/2(N+1/2)^2$. The two-dimensional states of the hydrogen atom and of the smoothed model atom are also numerated by the magnetic quantum number μ $(-N<\mu<N)$ corresponding to rotations by an angle α in the x-z plane; in the latter case the energies for a fixed N decrease for growing $|\mu|$. For a 1D smoothed potential there is no degeneracy and the energy for large n behaves as $E_n\sim-1/2n^2$. If the 1D potential becomes singular $(a=0)$, a degeneracy of even and odd states occurs, with the former having a discontinuous derivative and its energies are equal precisely $E_n=-1/2n^2$. In the 3D case we used the standard textbook hydrogen solutions expressed in the cylindrical coordinates, with the part dependent on φ being constant due to the assumption that $m=0$.

In order to obtain bound states of the smoothed model atom we used our implementation of the Davidson method [19] to solve the stationary Schrödinger equation. This method is very effective in comparison with other methods, especially in two dimensions, if one is interested only in a not too large number of lowest bound states. In our case the matrix to be diagonalized is obtained by the discretization of the Hamiltonian. In the 2D case the states with $\mu=0$ (μ is the quantum number connected with the rotation in the x-z plane described by the angle α) were calculated on a full 2D grid with 2×10^{11} nodes and the range $(-200,200)$ a.u. in both directions. The radial parts of the wave functions of the states with $|\mu|>0$ were calculated on a grid with 2×10^{13} nodes and the range (0,200) a.u. For all 3D states we took 2×10^{14} nodes in the range (0,300) a.u. The angular part is given by $e^{i\mu\alpha}$ in two dimensions and Legendre polynomials $P_l(z/\sqrt{s^2+z^2})$ in three dimensions. The convergence of both calculations was carefully checked. For the 1D model atom the bound states were calculated using the shooting method. Selected results were confirmed using the Davidson method.

Applying the Davidson method we have also found the bound states of the 1D and 2D KH wells (for various ε_0), which is given by the general formula

$$V(x,y;\varepsilon_0) = \frac{1}{T}\int_t^{t+T} V(x-\beta(t),y)dt, \qquad (7)$$

where $\beta(t)$ is the electron classical trajectory in its oscillatory motion, possibly including also a slow movement of the turning points. The above integral can be calculated numerically for the smoothed atom potential, while for the potential with a singularity it is divergent. The position of the original binding potential in the electron frame is additionally adjusted to the current position of the wave packet in the laboratory frame. The shapes of KH potential, even for a model smoothed potential, make it difficult to obtain the bound states using usual methods (in particular the shooting method, often used for 1D potentials, is useless in this case). The one-dimensional bound states were found on a grid with 2×10^{14} nodes and the range $(-100,100)$ a.u., and the two-dimensional ones were found on a grid similar to that used for a smoothed model atom. However, the Davidson method failed while calculating the eigenstates of the three-dimensional KH wells for $m=0$ (it works better for $m>0$). Including the additional singular term in the potential causes a numerical instability of this method, as well as of the Arnoldi algorithm [20], which we tested for this purpose. After all we managed to obtain only eight eigenstates of the three-dimensional KH wells for values of electric field intensity in the range between 1 and 5 a.u. using the one-electron diatomic states method [21]. This method is generally designed

for calculating the ground states of once ionized diatomic molecules (for example, of H_2^+). The excited states can be obtained by extracting the earlier computed states from the Hilbert space being used by the program. Thus the number of states one is able to calculate is rather limited and its energies should be well separated.

D. Determination of the wave-packet evolution

The dynamics of the recombination has been examined by a numerical integration of the time-dependent Schrödinger equation. In the 1D case we used the Crank-Nicholson scheme, while for the 2D and reduced 3D cases we used the *alternate-direction implicit* (ADI) algorithm [22].

It must be stressed that despite the 2D character of calculations, our 3D results are not approximated. Unfortunately only the systems with an axial symmetry may be treated in above described way. Another approach allowing a treatment of the arbitrary 3D system with quasi-2D simulations is the close-coupling algorithm developed by Geltman [23] and widely used by Hansen *et al.* [24], who used it to simulate the real hydrogen atom. In this method the dynamics of the wave function is calculated using the basis of eigenstates of the binding potential. Thus this method is generally limited to systems in which both the bound states and continuum states are explicitly known. For other algorithms see [25] and references therein.

One-dimensional computations for the hydrogen atom which are numerically inconvenient because of the singularity have been performed on the spatial grid as large as 2×10^{16} nodes. The space covered by this grid extends from -400 to 400 a.u. (the grid step is about 0.0122 a.u.). The wave-packet evolution was calculated in 62 000 time steps, each equal to $\pi/10^4$ a.u., which cover three optical cycles. The convergence was confirmed for the largest electric field used in the simulations with a ten times smaller time step. The smoothed model atom requires a less dense spatial grid but we used the grid with the same step to make the analysis easier. Two-dimensional simulations were performed for the singular hydrogen atom on the grid with 2×10^{11} nodes and the range $(-100,100)$ a.u. in both directions. The evolution for the smoothed model atom was calculated using the grid with a twice larger space range. The convergence was checked on the grid with 2×10^{12} nodes. In the three-dimensional case, for both types of potential classes, the grid was constructed with 2×10^{10} nodes in the s direction for the range (0,100) and with 2×10^{11} nodes in the z direction for the range $(-100,100)$. A higher density of nodes is recommended because of the strong singularity in $s=0$ introduced by the additional potential term.

III. RESULTS

We have chosen the sum of the populations of the bound states as a most reliable measure of the efficiency of the recombination. It will be called simply the recombination level or the atom survival probability. The most interesting feature is the dependence of this quantity on the amplitude of the laser field, and as a consequence, on the details of the slow drift. In addition it seems important to examine whether the recombination level depends on the potential type used in our simulations. As will be demonstrated in detail below, the result of our studies is that for the 2D and 3D hydrogen singular potentials, a nonmonotonic dependence of the recombination level on the laser field intensity may be observed, i.e., the phenomenon analogous to the stabilization in the ionization process is present, while it is absent for the smoothed model atom (see Figs. 1 and 7 for comparative plots). However, this phenomenon in two dimensions is much better pronounced than in the 3D case.

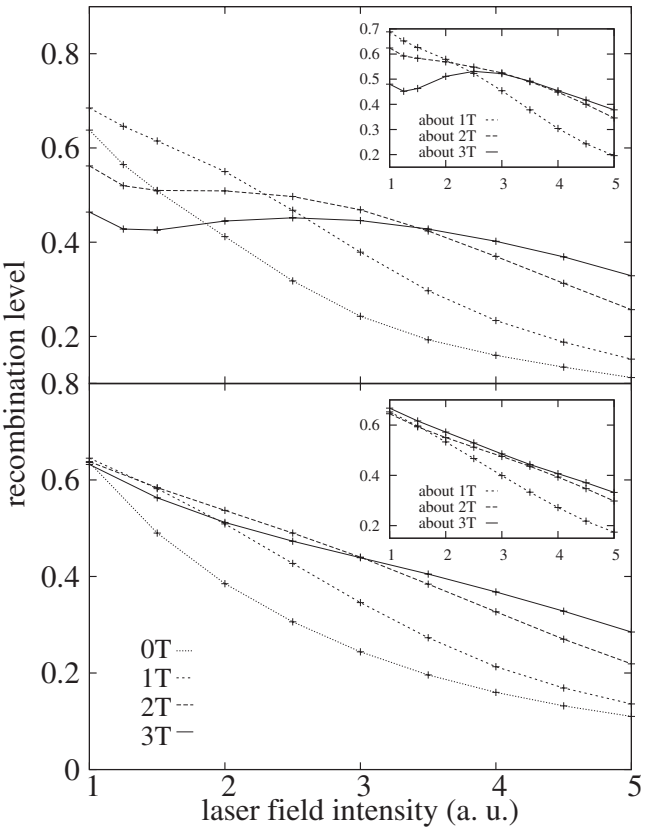

FIG. 1. The final level of the recombination (sum of the populations of a few lowest bound states) as a function of the electric field intensity in the case of the real hydrogen atom (upper plot) and the 3D smoothed model potential (lower plot). The populations were calculated after exactly one, two, and three optical cycles except for the insets which correspond to time instants at which the sum of the populations exhibits a local maximum. Also shown are the initial total populations of the bound states, the values of which are not negligible due to packet being initially not very far from the nucleus. The abbreviation a.u., used in this figure as well in the next ones, stands for atomic units.

In one-dimensional simulations the opposite results were obtained. A nonmonotonic dependence of the recombination level appears for a smoothed model atom while it is absent or less pronounced for the Coulomb potential. It is important to keep in mind that in the 2D case a monotonic behavior of the recombination level as a function of the laser field was predicted for a short-range potential, in contrast to the 1D case [9].

A. Results for the 3D case

The dependence of the recombination level on the laser field intensity in the case of the real hydrogen atom is shown in the upper plot of Fig. 1. It is nonmonotonic for $t=3T$, although the first symptoms of creating the stabilization window for $\varepsilon_0=1.5-2.5$ a.u. are visible already at $t=2T$ and $t=2.5T$ (the latter is not shown). Note that the initial population of the discrete states is nonzero because of the overlap of the packet with some excited states. The total population of bound states at $t=0$ given by the dotted line is field dependent because of the field dependence of the packet initial position. At any rate this initial dependence is monotonic. The flat maximum in the recombination level for longer pulses becomes more clearly visible if one compensates the influence of the slow drift on the recombination, which may be done by calculating the populations after the laser pulse has been switched off not exactly after an integer number of cycles but at the close instants when the recombination level has reached the highest value (see [9,10] for a detailed explanation). The insets of Fig. 1 present the recombination level for the 3D Coulomb potential obtained in such a way. The nonmonotonic behavior of the recombination level seen in the insets suggests that for 3D real hydrogen atom, the stabilizationlike phenomenon is caused mainly by trapping the population in a sort of the KH well and the slow drift plays not very prominent but rather a destructive role.

However, one should be cautious using the notion of the KH well in the context of the singular potential because integral (7) defining the KH potential, which describes an average of the original binding potential moving in the electron frame during the one optical cycle, is divergent in this case; thus it is not possible to calculate the populations of its bound states. However a sort of trapping definitely occurs in the sense that a part of the packet does not leave the vicinity of the nucleus.

In contrast to the case of an atom with a singularity, a nonmonotonic behavior cannot be observed for few-cycle pulses in the case of the 3D smoothed model atom. The recombination level systematically decreases for a growing electric field (see the lower plot of Fig. 1). Comparing the lower plot of Fig. 1 and its inset, that is, the population of the eigenstates of the smoothed model atom perturbed and not perturbed by the slow drift, one may conclude that in the three-dimensional case of the smoothed model atom the values of the recombination level are not disturbed by the slow drift; thus it should depend solely on the amount of population trapped in the KH well bound states. To check this we have calculated the total population of the bound states of the KH wells for various electric field intensities. It is shown in Fig. 2. Indeed the values of the KH well total bound-states' population are very close to those of the population of the bound states of the original potential (lower plot of Fig. 1). This is not the case in one and two dimensions, where the influence of the slow drift is more significant.

We have checked that only the populations of a few bound states with lowest energies (of both potentials) are significant during the recombination process. Figure 3 shows that the populations of higher excited states are much smaller than the population of the ground state and of a few lowest excited states. It encourages one to believe that limiting ourselves to nearly 15 states with lowest energies is a good approximation for calculating the recombination level. The same applies to the eigenstates of the KH wells.

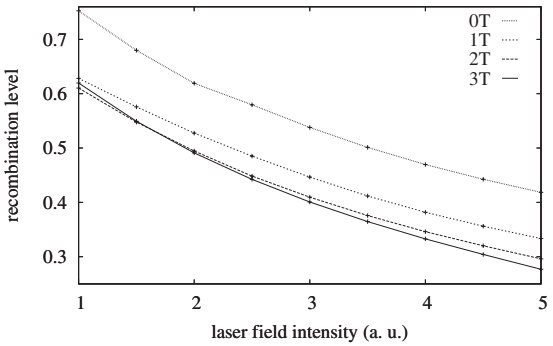

FIG. 2. The sum of the final population levels of the KH states depending on electric field intensity in the case of the 3D smoothed model potential. The populations were calculated at the same time instants as in the previous figure.

We have also calculated the probability (not shown) of finding the electron close to the nucleus, given by an integral of the square modulus of the wave function over $(-2\varepsilon_0-\Delta,\Delta)$ a.u. in the z direction and $(0,\Delta)$ a.u. in the s direction. It is often considered as an approximation to the survival probability, especially if the eigenstates of the potential are not available. In our calculations we have taken $\Delta=5$, which seems a reasonable characteristic length, on which the results only weakly depend. Our result is that this probability is monotonic in both cases and decreases with a growing field intensity. This means that in the 3D case this approximation does not work well. As we will see below, it works much better in the 2D and 1D cases.

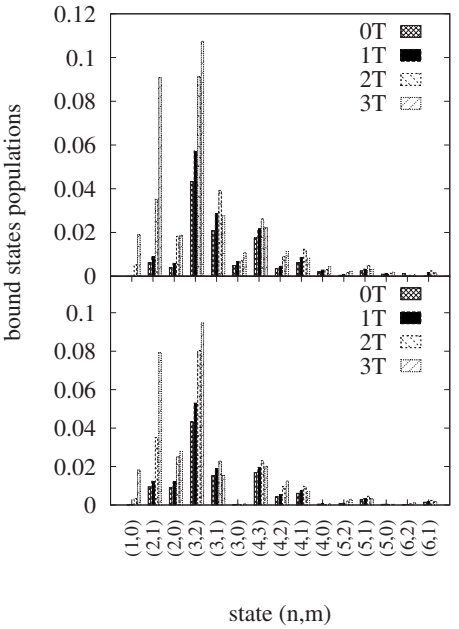

FIG. 3. The population of a few lowest bound states for $\varepsilon_0=5$ a.u. in both studied 3D cases (singular potential, upper plot; smoothed potential, lower plot) ordered according to growing energy.

One may interpret the differences of the recombination levels for the two classes of potentials (or the corresponding ionizations levels) as differences of a more physical nature. If one assumes that the smoothed model atom better imitates the case of a massive nucleus (and thus of a larger "core"), then one may claim that relatively light ions exhibit a nonmonotonic dependence of the recombination level on the laser field intensity while the heavy ones have no such property.

It should be stressed that during the ionization in the regime of superintense laser fields, it is difficult to separate the recombination and ionization processes. Both occur simultaneously. Even for usual ionization, i.e., when the initial packet is chosen as the ground state of the binding potential, the oscillatory motion of the released electron causes the backscattering that is always accompanied by the recombination already at the first cycle of the electric field. This leads to the characteristic comblike shape of the total occupation level. One finds a similar behavior for recombination, although many aspects of the dynamics of the two processes differ much.

In our simulations the initial position of the electron was fitted to the electric field applied to the electron by setting $z(T/2)=0$. In an almost free-electron regime it leads to $z(0)=-2\varepsilon_0/\omega^2$. The idea was to perform simulations for such an electron from a whole beam for which the probability of an efficient recombination after half a cycle is largest. One should however keep in mind that the packet will adjust to the shape of new dynamically binding potential, i.e., the KH well [6], by shifting toward the center of this well. As a consequence the maximum of the occupation of the bound states as the function of the initial position z_0 shifts toward smaller values (not shown). Unfortunately it happens during the time of a few cycles, so even the attosecond regime does not protect against it. Moreover, for longer pulses the idea of choosing the initial position, taking into account this shift, is also in vain because of the slow drift phenomena appearing for longer times.

Due to the long-range potential the initial occupations of some excited states in our simulations are significantly larger than zero. However, we are rather concentrated on the dependence of the recombination level on ε_0 (exposing the stabilizationlike phenomena) rather than on the recombination efficiency itself. Furthermore one can lower the initial population by shifting the initial position of the electron toward the direction opposite to the nucleus. The total occupation at $t=0$ (initial) depends stronger on the initial position shift than that at later times, at least for the shift in the range between z_0-2 and z_0+2 a.u. (not shown).

Additionally, doubts may arise whether the effect visible for such restrictive initial conditions may survive in experimental conditions in which the velocity and the position of the electrons in the beam vary. Thus we also varied the initial position of the electron by 1 and by 2 units in both directions along the x axis for each electric field intensity. (In the oscillating motion this averaging is also equivalent in some sense to varying the velocity.) For $t>1T$ the total recombination level, dependent on the initial position, changes almost monotonically in the range of (z_0-2,z_0+2); thus the averaged results are close to the original ones obtained for

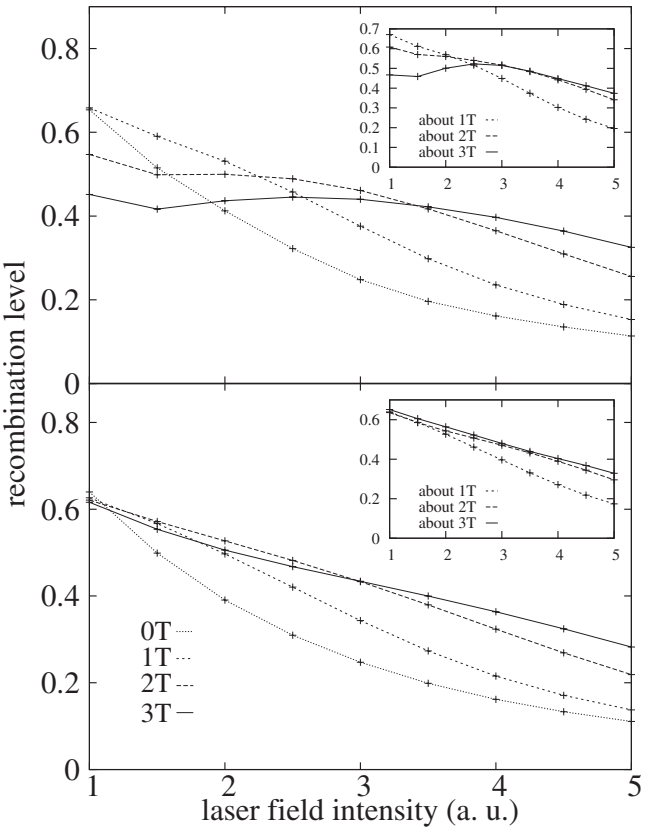

FIG. 4. The final level of the recombination as in Fig. 1 but averaged over the packet initial positions $[z_0(\varepsilon_0)-1,z_0(\varepsilon_0)+1]$ for all values of ε_0; singular potential, upper plot; smoothed potential, lower plot.

default initial positions (see Fig. 4). As was discussed earlier, a monotonic dependence of the total bound-states' population during the recombination occurs in a wide range of the initial positions because the maximum of total recombination level as a function of the initial position is shifted by about 2 a.u. from z_0 toward the nucleus because of the phenomena of adjusting the wave packet to the shape of the KH well.

We have also performed some tests in which the initial position shift was compensated by an initial packet momentum. The results of those simulations were similar to the one, in which the initial position shift was not compensated. This is because the compensation is actually effective only at $t=0.5T$. It does not help for larger times.

As it was already mentioned, in the three-dimensional case the slow drift plays a less important role in forming the stabilization window than in one- and two-dimensional ones. It is however present, especially in the case of potentials with a singularity. Such potentials more strongly influence the wave function. It is also reflected in the wave-packet structure. Figure 5 shows the modulus square of the wave function after $3T$ for various electric field intensities. The left-hand plots show the cases of the Coulomb potential; the right-hand ones show the cases of the smoothed model atom. The general shape of both families of the wave packets is similar, but a more developed wave-packet structure is created in the case of the singular potential. One can recognize in it the so-called double-ring structure noticed by us earlier

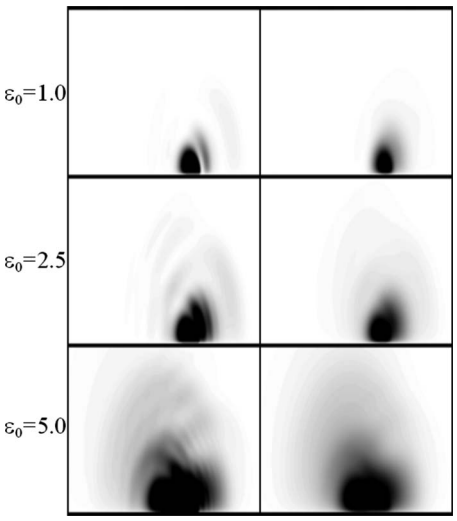

FIG. 5. The wave function in the z and s coordinates (transformed back to the standard cylindrical coordinates, i.e., divided by $\sqrt{s}$) for $t=3T$ and for various laser field intensities. The spatial range of the images is $(-30,15)$ a.u. in the z direction and (0,17) a.u. in the s direction. The blackness of the plot is proportional to the square of wave-function modulus. The case of the singular hydrogen potential is presented in the left-hand side, and that of the smoothed model potential is in the right-hand side.

in 2D simulations [7]. It is caused by different ionization and recombination rates depending on whether the wave packet currently rests at the center of the potential or it is far from scattering center and/or moves. This structure oscillates in the rhythm of the electric field. It has the form of two sets of concentric rings, each for the corresponding turning point. In three dimensions it has the shape of spheres; the intersections of which for any φ give the shape of rings visible at Fig. 5.

Some additional information on the 3D wave-packet dynamics and its slow drift may be gathered from the final expectation value z_f of the position and from the position of maximal value of the probability density of the wave packet, i.e., the position in which the probability of finding electron is largest (not shown). In Fig. 6 the expectation values of the wave-packet z position after an integer number of cycles and after an odd number of half cycles are shown. In the case of the singular hydrogen atom some deviations from the initial position which depend on laser field intensity may be observed after an integer number of cycles and from $z=0$ for an odd number of half cycles. It is most noticeable for $\varepsilon_0=2$. Moreover for both types of the potential this position gradually shifts toward the positive values of z according to the adjusting of the wave packet to the KH well shape (very short pulses end before this process has been finished). However, as mentioned earlier, in the regime of such short pulses this drift in the 3D case does not influence much the process of creating the stabilization window. The plots of the maximum of the probability density of the wave packet generally coincide with the plots of the expectation value, except for an integer number of cycles and simultaneously for ε_0 in the range between 3 and 4 for which the maximum switches to the $z=0$ (the other minimum of the KH well).

The expectation value of the electron position is very sensitive to any numerical inaccuracy. Thus it is advisable to

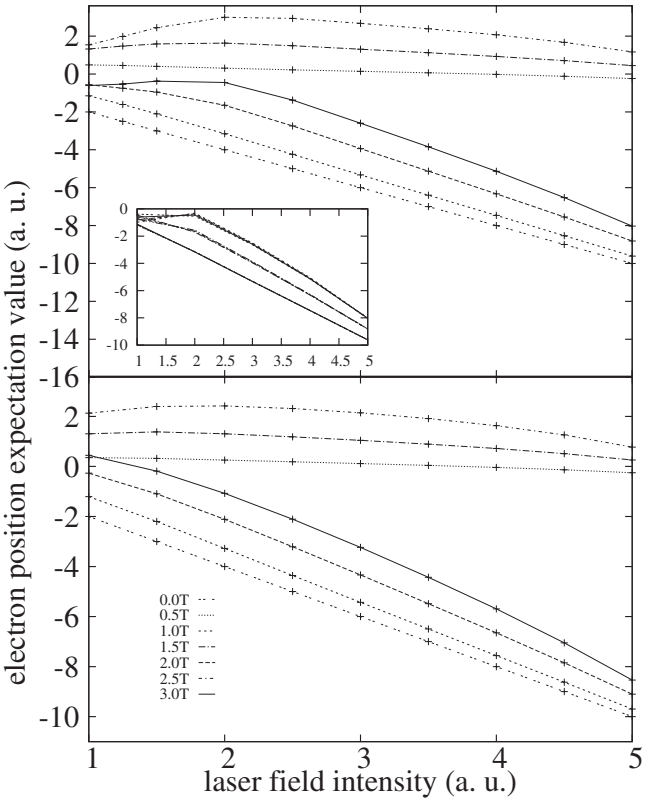

FIG. 6. The final expectation value of the position z_f of the 3D wave packet as a function of the laser intensity ε_0. The position of the wave packet after an odd number of half cycles should be close to zero if the slow drift were absent; the position after a full number of the cycles should be close to $z_0=-2\varepsilon_0/\omega^2$ in such a case. Any deviations from that pattern reveal the presence of the slow drift. The inset of the upper plot shows, for the potential with the singularity, the series of plots of $\langle x\rangle$ after full cycles for various grid steps and for the same space range (from 1024×512 up to 8192×4096). Except for the largest grid step the differences are almost indistinguishable.

check whether the results are independent on numerical details, especially on the space range and the grid or time steps. The last test was already described in Sec. II D. The space range was tested by taking a twice larger range with the same grid and time step. The results were the same. Also changing the grid step (number of nodes with the unchanged space range) does not influence the results much, at least for $\varepsilon_0>2$. The computed position expectation value converges already for the grid settings used for all calculations in this paper (see the inset of Fig. 6).

B. Results for the 2D case

The general results for the 2D cases are similar to the ones obtained in 3D simulations, but the stabilizationlike behavior of the recombination level for the potential with singularity is more prominent. The recombination level dependent on the laser field intensity in the case of the 2D hydrogen atom is shown in the upper plot of Fig. 7. Its behavior varies at various stages of the recombination process. After $0.5T$ (not shown), i.e., at the time instant of the first

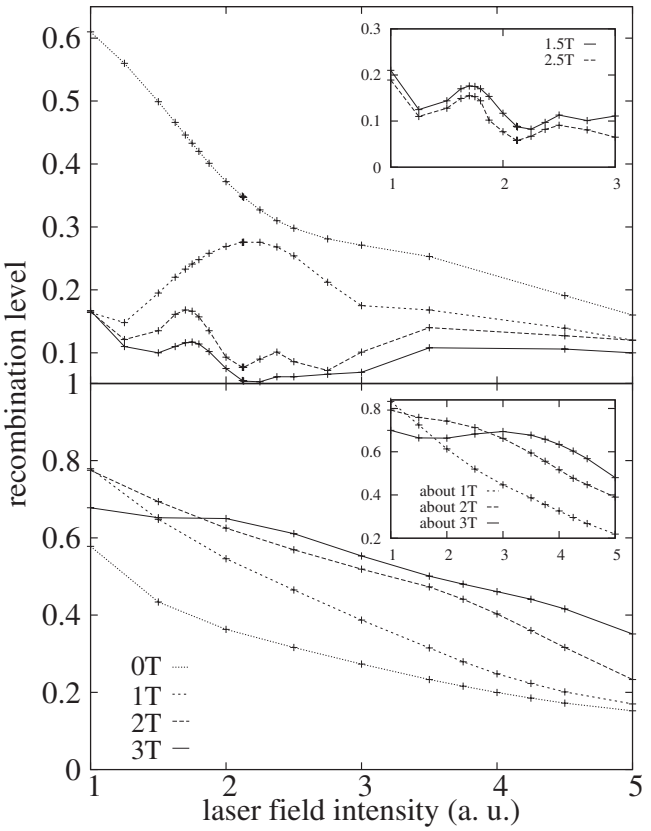

FIG. 7. The final level of the recombination as a function of the electric field intensity in the case of the 2D hydrogen atom singular potential (upper plot) and the 2D smoothed model potential (lower plot). The populations were calculated at initial moment as well as after exactly one, two, and three optical cycles, except for the inset in the lower plot which is prepared for time instants at which the sum of the populations exhibits a local maximum. The inset in the upper plot is prepared exactly for $1.5T$ and $2.5T$.

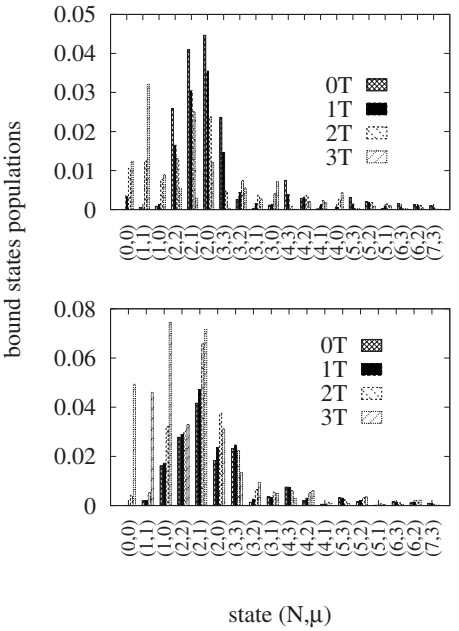

FIG. 8. The population of a few lowest bound states for $\varepsilon_0 = 5$ a.u. in both studied 2D cases (singular potential, upper plot; smoothed potential, lower plot) ordered according to growing energy. Higher states are less populated thus the truncation to a few lowest states is justified.

contact of the incoming wave packet with the nucleus, there is no nonmonotonicity—the recombination level systematically grows, at least in the range of ε_0 between 1 and 5 a.u. After $1T$, i.e., when the broadened wave packet returns in the vicinity of its initial position, the level reveals a relatively large maximum for $\varepsilon_0=2.25$ a.u. At later times ($2T$ and $3T$ shown in the upper plot and $1.5T$ and $2.5T$ shown in its inset), the maximum shifts to $\varepsilon_0=1.75$ a.u. and significantly decreases. At the same time after an integer number of the optical cycles a wide minimum in atom survival probability appears for values of ε_0 between 2 and 3.5 a.u.

Similarly as in the 3D case such a nonmonotonic behavior of the recombination level is absent for the smoothed model atom (see the lower plot of Fig. 7) although its value is generally twice as large as in the case of the singular hydrogen atom. We have also calculated this quantity, compensating the slow drift. The inset in the lower plot of Fig. 7 presents the recombination level for the smoothed model atom calculated in such a way. It corresponds well to the population of the sum of the KH well bound states discussed below (cf. Fig. 12). One can see that this procedure reveals only a slight minimum, which appears around $\varepsilon_0=1.75$ a.u. at $t_f \approx 3T$. However, the slow drift, which shifts the wave packet toward the nucleus ($z=0$) for this value of the laser field intensity, cancels this minimum in the case of exactly $t_f = 3T$ (see below for additional comments on the slow drift).

We have checked whether the populations of the bound states in the 2D case tend to zero for a growing energy. In addition to the states presented in Fig. 8 we have checked that the sum of populations of additional 13 states (not shown) is smaller than 0.006 and thus negligible.

The difference between the results obtained for the singular hydrogen atom and for the smoothed model atom is even more distinct for time-dependent quantities. As an example we present in Fig. 9 the time-dependent recombination level for both potentials. Please note that a more complex structure of the time-dependent recombination level in the case of the singular hydrogen atom is related to a more complex polymorphic structure of the wave function, i.e., the already mentioned double-ring structure [7] which is much more prominent in the case of the singular hydrogen atom that is visible in Fig. 10 (see also the description below).

In contrast to the 3D case the recombination level in 2D presented in Fig. 7 should be considered as dependent on both the populations of the bound states of the KH well corresponding to the used binding potential and the slow drift of this well (and thus of the electron wave packet) which occurs in the range of $(-2\varepsilon_0/\omega^2,0)$ (cf. [9,10]). This slow drift, much more prominent in the 2D case than in the 3D one, is due to the interaction of the quickly oscillating packet with the binding potential. The turning point of the slow drift occurs when the packet performs a quick oscillation without passing the nucleus, i.e., remaining on its one side. Figure 10 presents a few snapshots of the wave function taken after an integer number of the optical cycles. The drift

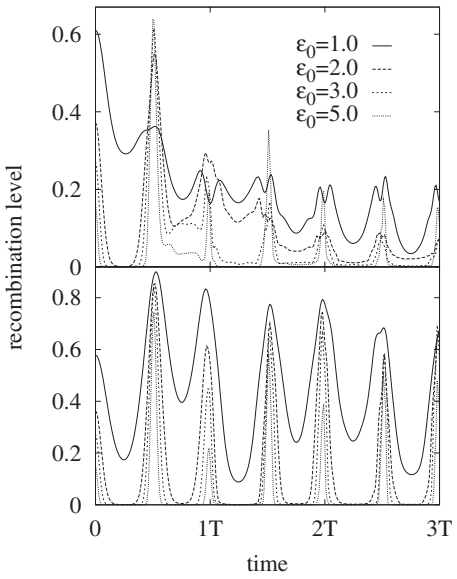

FIG. 9. The dynamics of the sum of the populations of a few lowest bound states in the singular hydrogen atom (upper) and smoothed model atom (lower). A more complicated structure of the recombination level in the former case is caused by a better developed double-ring structure of the wave function.

of the expectation value of the packet position toward the center of the binding potential along the z axis is clearly visible. Because of the attosecond regime of the pulse duration this slow drift has no chance to reveal its oscillatory character as was observed in longer simulations [6,10]. The process of forming the KH well is also visible together with

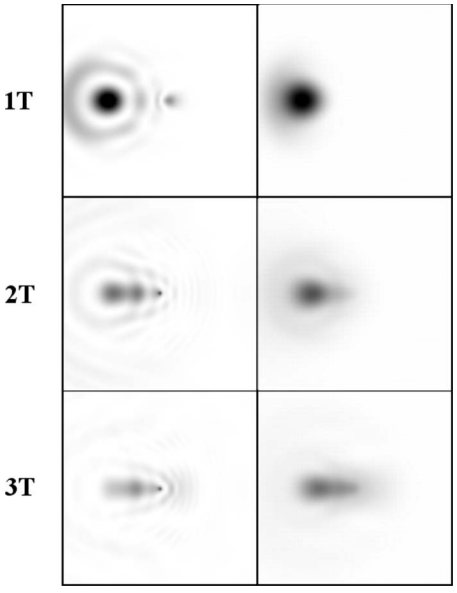

FIG. 10. The evolution of the 2D wave function for $\varepsilon_0=5$ a.u. presented in three snapshots calculated for $t_f=1T$, $2T$, and $3T$. The spatial range of the images is $(-15,15)$ a.u. in both directions. The blackness of the plot is proportional to the square of wave-function modulus. The case of the singular hydrogen potential is presented in the left-hand side, and that of the smoothed model potential is in the right-hand side.

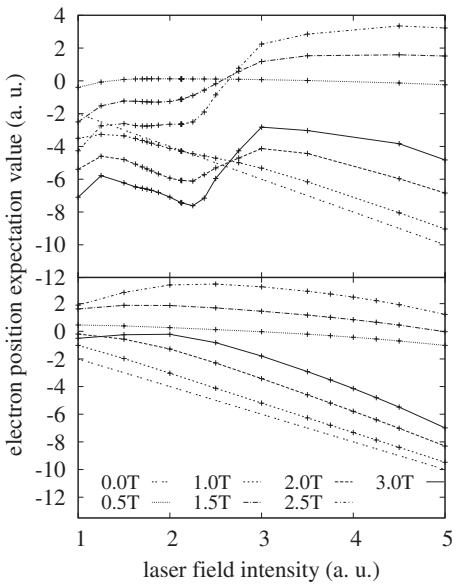

FIG. 11. The final expectation value of the position z_f of the wave packet as in Fig. 6 but for 2D; singular potential, upper plot; smoothed potential, lower plot.

the double-ring structure caused by the scattering on the nucleus. The effect of scattering is strongest when the packet temporarily rests, which occurs twice a period; this leads to the already mentioned double-ring structure (cf. [7]). Similarly as in the 3D case, this structure is much better visible for the hydrogen atom because of its singularity which creates a more effective pair of the scattering centers in the KH picture.

The case of a relatively low laser field intensity ($\varepsilon_0=1.0-2.0$ a.u.) is especially difficult to interpret since both the forces due to the binding potential and due to the external electric field are comparable. A fully reliable model for this case is unavailable. More complex double- and triple-peak structures of the time-dependent recombination level visible at the upper plots of Fig. 9 for $\varepsilon_0=1.0$ and $\varepsilon_0=2.0$ a.u. are caused by an interplay of the two phenomena: a polymorphic structure of the wave function rescattered on the singular binding potential and an additional velocity which reduces the total bound-states' populations and is due to the slow drift (it also shifts in time the instant of reaching the turning point). It is well visible at the movie presenting the series of the wave-function snapshots for a singular atom potential, available in Ref. [26].

The presence of the slow drift in the 2D case is also confirmed by Fig. 11, which shows the expectation value of the position z_f at the instant of switching the pulse off after a given time ($t_f=0.5T-3T$). The elimination of the slight stabilization window in the recombination level of the smoothed model atom has already been discussed. In the case of singular potential the dependence of the z_f on the ε_0 looks more dramatic. At the same time a comparison of the recombination level calculated with and without compensating the slow drift (the latter is not shown) convinces one that the slow drift influence on the recombination level for $\varepsilon_0<3$ is less evident; both plots look much the same in this range of laser intensities. It is because in this case the value

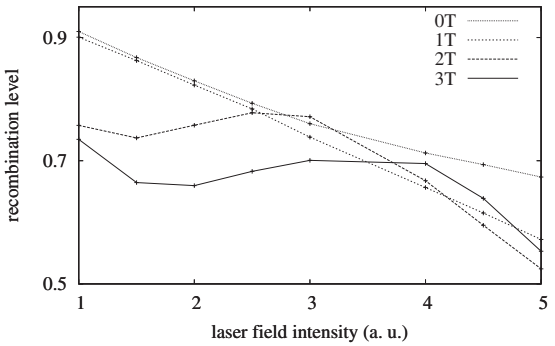

FIG. 12. The sum of the final populations of the 2D KH well ten lowest bound states as a function of the electric field intensity, cf. Fig. 2.

z_f is strongly modified by the ionized parts of the wave packet creating the double-ring structure, and thus this quantity does not reflect well the slow drift of the trapped part of the wave function. However, for $\varepsilon_0 > 3$ the slow drift significantly lowers the value of the recombination level.

It is possible to calculate the population of the KH well in the case of the smoothed model atom (Fig. 12). In the range of ε_0 between 1.0 and 5.0 a.u. it is monotonic for $t=1T$, but for $t=2T$ and $3T$ slight maxima appear at $\varepsilon_0=2.75$ and $\varepsilon_0=3.5$ a.u., respectively. This corresponds to the position of a slight maximum visible for the recombination level of the smoothed model atom after taking into account the influence of the slow drift—see the inset in the lower plot of Fig. 7. Notice that in the 3D case the dependence of the sum of the KH well bound-state occupation level on the strength of the laser field is monotonic for all laser-pulse lengths used in our simulations.

As we have noticed earlier, it is not possible to calculate the KH well for the singular hydrogen and in consequence its total bound-states' populations are not available either. One can however estimate an analog of the total population of the KH well or rather the trap with an infinite depth placed in the area of the free oscillations, taking into account also the slow drift, by calculating the probability of finding the electron in the corresponding area, i.e., $(z_f-\Delta, z_f+2\varepsilon_0/\omega^2+\Delta)$ in the z direction and $(-\Delta, \Delta)$ in the x direction (not shown). After $1T$ it is almost constant with a small local maximum at $\varepsilon_0=2.25$ a.u. It corresponds to the maximum at the recombination level for $\varepsilon_0=2.25$ a.u. after $1T$, visible in Fig. 7 (upper plot). For $t=3T$ another local maximum appears at $\varepsilon_0=1.75$ a.u., the position of which corresponds to the position of the maximum in the recombination level after $2T$ and $3T$, also visible in Fig. 7 (upper plot).

C. Results for the 1D case

There is a long tradition of using the smoothed model-atom potential in one-dimensional simulations of strong laser field interaction with atoms since it was proposed by Su and Eberly in 1991 [16]. Warned by the discrepancies revealed by 2D and 3D simulations we decided to revise also the applicability of 1D smoothed model atoms for the simulations of the recombination process. The comparison of the

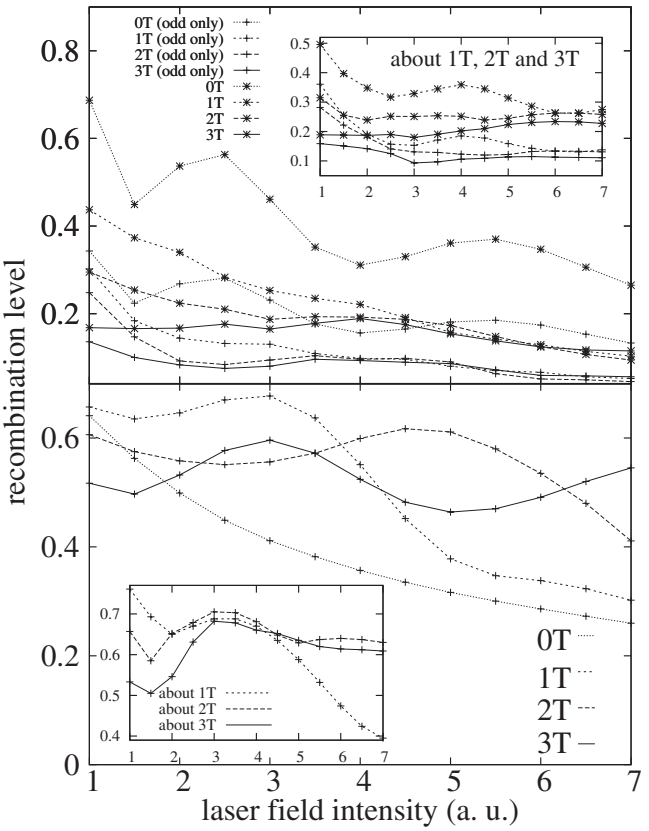

FIG. 13. The final level of the recombination as in Fig. 7 but for 1D; singular potential, upper plot; smoothed potential, lower plot.

recombination levels for both potentials in the 1D case as a function of the laser field intensity is shown in Fig. 13 (again the upper plot presents the results for the singular potential, and the lower one presents the results for the smoothed potential). From the figure it follows that the exact shape of the potential function around $z=0$ is also very important in one dimension and the obtained results significantly differ in both cases, namely, an analog of the stabilization appears for the case of the smoothed model atom while it is absent in the case of the singular atom potential. This might suggest that some of the so-far-published results for a smoothed potential could be uncertain or at least their applicability is limited to rather heavy atoms with soft-core nuclei.

The study of the recombination of the electron in the presence of the long-range 1D potential was already published by us in [10] but it was limited only to the smoothed model atom. Moreover, the recombination level in [10] was roughly estimated by calculating the ground-state population only, which might not be precise enough (cf. the lower plot of Fig. 13 with Fig. 1 of Ref. [10]). Figure 14 presents the particular final populations of the eigenstates after $3T$ and also confirms that in one dimension the truncation of the number of states in the calculation of the recombination level in this paper is justified but restricting ourselves to a single ground state in [10] was not sufficient. The inset of the upper plot shows again the importance of both odd and even states in the case of the singular hydrogen atom potential.

Similarly as in the 2D case, the recombination level in the smoothed model atom is about twice as high as in the singu-

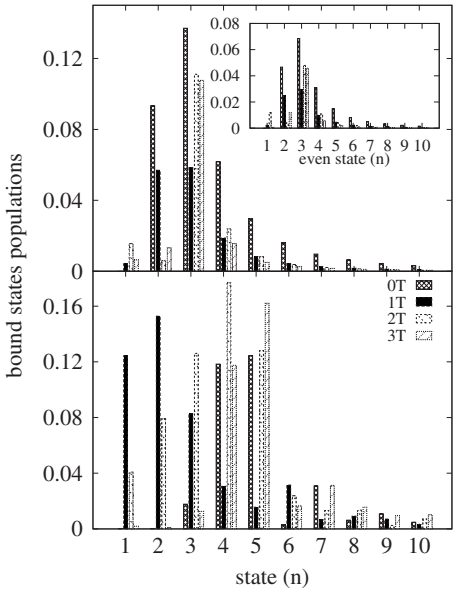

FIG. 14. The populations of the bound states as in Fig. 8 but for 1D. The sum of populations of the odd and even states is drawn for the singular hydrogen atom (upper plot). The inset of this plot presents the populations of only even states.

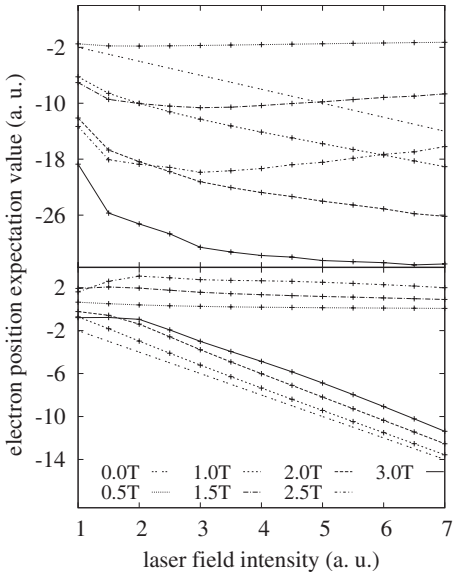

FIG. 15. The final mean positions of the wave packet as in Fig. 11 but for 1D; singular potential, upper plot; smoothed potential, lower plot.

lar hydrogen atom. However, in the 1D singular hydrogen atom one should be more careful while choosing the eigenstates, the population of which should be summed up. Because of the singularity of the potential all eigenvalues are degenerate (every energy level has two corresponding states with odd and even parities), and there is no agreement about building the complete bases in this case as was described in Sec. II. The upper plot of Fig. 13 shows three sets of pairs of lines drawn with the same style (dotted for $t=1T$, dashed for $t=2T$, and solid for $3T$); the upper line is calculated for both the even and odd states, while the lower one is only for the odd states. It is clearly visible that the population of the even states is comparable with population of the odd ones. Thus one may claim that both odd and even states take part in the electron evolution.

The electric field range, for which a wide maximum of the atom survival probability (see Fig. 13) occurs in the recombination process in the case of the smoothed model atom, essentially varies in time. For $t=1T$ and $t=3T$ the maximum lies at about $\varepsilon_0=3$ a.u., while for $t=2T$ it is located at about $\varepsilon_0=5$ a.u. This is caused by the slow drift even if it is not very prominent (see the lower plots of Fig. 15). It shifts in time the instant at which the recombination level takes its local maximum (note that the peak around this local maximum is very narrow); thus it is useful to measure the recombination level exactly at the moment at which this maximum occurs, i.e., at which there is no influence of the slow drift on the atom survival probability (compare a similar plot in the 2D case presented in the inset of the lower plot of Fig. 7). It is shown in the inset of the lower plot of Fig. 13. In the case of the smoothed model atom such a procedure leads to obtaining a single value of the laser field intensity for which a maximum of the recombination level occurs. The only maximum is now located around $\varepsilon_0=3$ a.u., which agrees with the dependence of the total population of the eigenstates of the KH well on the electric field intensity presented in the inset of Fig. 16 as well as the probability $P(z_f)$ of finding the electron in the vicinity of the nucleus [namely, at an area of $(z_f-\Delta, z_f+2\varepsilon_0/\omega^2+\Delta)$] presented at the lower plot of Fig. 16. To conclude, one may claim that in the 1D case the dependence of the recombination level in smoothed model atom is generally determined by the dependence of the population of the eigenstates of the KH well but it can be strongly modified by the slow drift, if one measures the recombina-

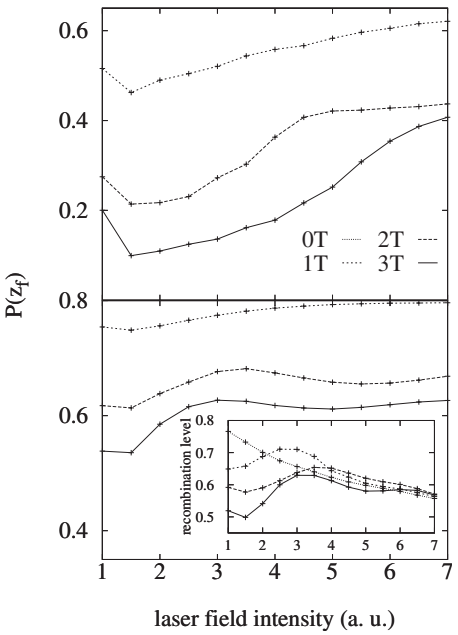

FIG. 16. The probability of finding the electron in the vicinity of the nucleus as a function of the electric field intensity; the singular potential, upper plot; the smoothed potential, lower plot. In the inset: the sum of the final populations of the 1D KH well ten lowest bound states as a function of the electric field intensity.

tion at a fixed time, even if the drift amplitude is not very large. Thus in the context of the influence of the slow drift the 1D case of the smoothed model atom is similar to the 2D case and not to the 3D case in which the slow drift does not disturb the final populations much.

The case of the 1D singular hydrogen atom is more difficult to interpret since it is not possible to calculate the corresponding KH well. Instead we again calculate the probability $P(z_f)$ of finding the electron in the vicinity of the nucleus (as explained above) presented at the upper plot of Fig. 16. It is a growing function of ε_0 which suggests the presence of the stabilizationlike phenomenon. However, the slow drift, which is much stronger in the case of the singular potential than in the case of the smoothed model atom, causes the recombination level visible at the upper plot of Fig. 13 to be a decreasing function of ε_0. Thus the slow drift eliminates stabilization in this case, especially when the recombination level is calculated after exactly full cycles. Only for $t=3T$ a slight and relatively wide maximum is seen at $\varepsilon_0=4$ a.u.

Changing the value of parameter a in Eq. (2) causes a gradual transformation of singular hydrogen atom potential into the smoothed model-atom potential. We have checked how the value of parameter a influences the final recombination level. It depends on the laser field intensity used in the recombination process; for higher intensities of $\varepsilon_0 > 3.5$ a.u. the recombination level changes monotonically. It changes more rapidly for $a < 0.25$ a.u. than for $a > 0.25$ a.u. For lower intensities the change is more irregular, especially for small values of a and long times $t_f \geq 2T$.

IV. CONCLUSIONS

In the present paper we have described the results for the electron recombination with the ion modeled by a long-range potential in one, two, and three dimensions in the presence of an ultrastrong attosecond linearly polarized laser pulse. We have discussed the differences stemming from the exact shape of those potentials, in particular from the presence of a singularity for Coulomb potentials or its absence for smoothed potentials, often used in model numerical studies. The recombination level has been analyzed in terms of the final populations of the bound states, the final probability of finding the electron in the vicinity of the nucleus, and when possible, in terms of the final populations of the eigenstates of the KH well.

A nonmonotonic dependence of the recombination probability on the field intensity, which is a counterpart of the stabilization against photoionization, has been discovered for a 3D hydrogen atom, described by the usual singular Coulomb potential, but surprisingly not for a model with a smoothed potential. However, one should be aware that our choice of the initial states used in the simulations, the positions of which depend on the laser field intensity and the projections of which on the atom excited states are not negligible, surely influences the details of the recombination process as well as the final bound-state occupations but not the general qualitative observation. A similar observation of nonmonotonicity of the recombination level is true for two-dimensional models. In the case of one-dimensional model atoms the situation is the opposite; the nonmonotonicity occurs for smoothed potentials but not for singular ones. This is due to the fact that in three and two dimensions the packet is allowed to broaden in the directions perpendicular to field amplitude and the packet fragmentation on a singular potential is not as strong as in one dimension. The effect of the packet slow drift has been shown to influence the final results but it is not responsible for the essence of the effect.

The manifestation of a nonmonotonic recombination probability as a function of the laser field intensity and the differences between the results for singular and smoothed potentials for one-, two-, and three-dimensional models are in our opinion the most important message of this paper. Taking into account the importance of the smoothed model-atom potential for quantum optics in ultrastrong laser regime, it is crucial to be aware of its limitation. In contrast to our earlier results obtained for relatively long pulses, the slow drift in the regime of few-cycle pulses is generally responsible rather for eliminating or reducing the stabilization phenomenon than for its creation. In addition we found that the states of the 1D hydrogen atom with even parity, sometimes considered as nonphysical, become populated which convinces one about their physical status.

ACKNOWLEDGMENTS

We would like to thank A. Raczyński and J. Zaremba for extensive and fruitful discussions and help in preparing this paper and J. Kobus for making available to us his code of the program we have used to obtain the eigenstates of the 3D KH wells. This work was partially financed by European Social Fund, the budget of Poland, and the budget of the Kujawsko-Pomorskie province as a part of the Operational Programme Human Capital Priority VIII, act 8.2, "Regional Innovations Strategy," the project Kujawsko-Pomorskie Province Government "Step in the future—grant for doctoral students," and by the Nicolaus Copernicus University under Grant No. 430-F.

[1] M. Drescher, M. Hentschel, R. Kieneberger, M. Uiberacker, V. Yakovlev, A. Scrinzi, Th. Westerwalbesloh, U. Kieneberg, U. Heinzmann, and F. Krausz, Nature (London) **419**, 803 (2002); M. Hentschel, R. Kieneberger, Ch. Spielmann, G. A. Reider, N. Milosevic, T. Brabec, P. Corkum, U. Heinzmann, M. Drescher, and F. Krausz, *ibid.* **414**, 509 (2001); A. Baltuska, Th. Udem, M. Uiberacker, M. Hentschel, E. Gouliemalmakis, Ch. Gohle, R. Holzwarth, V. S. Yakovlev, A. Scrinzi, T. W. Hänsh, and F. Krausz, *ibid.* **421**, 611 (2003).

[2] R. Kienberger, E. Goulielmakis, M. Uiberacker, A. Baltuska, V. Yakovlev, F. Bammer, A. Scrinzi, Th. Westerwalbesloh, U. Kieneberg, U. Heinzmann, M. Drescher, and F. Krausz, Nature

(London) **427**, 817 (2004); J. Itatani, F. Quéré, G. L. Yudin, M. Yu. Ivanov, F. Krausz, and P. B. Corkum, Phys. Rev. Lett. **88**, 173903 (2002).

[3] *Attosecond Research Could Aid Homeland Security*, in rt Image, Vol. 20 (28), p. 6 (2007), available online at http://www.rt-image.com/News_Extras/content=9204J05C48568A8640569A724480B0441

[4] M. V. Fedorov, *Atomic and Free Electrons In a Strong Light Field* (World Scientific, Singapore, 1997).

[5] J. H. Eberly, R. Grobe, C. K. Law, and Q. Su, in *Atoms in Intense Laser Fields*, edited by M. Gavrila (Academic, Boston, 1992), p. 301.

[6] J. Matulewski, A. Raczyński, and J. Zaremba, Phys. Rev. A **61**, 043402 (2000).

[7] J. Matulewski, A. Raczyński, and J. Zaremba, Phys. Rev. A **68**, 013408 (2003).

[8] J. Matulewski, A. Raczyński, and J. Zaremba, Phys. Rev. A **68**, 045401 (2003).

[9] J. Matulewski, A. Raczyński, and J. Zaremba, Eur. Phys. J. Spec. Top. **144**, 155 (2007).

[10] J. Matulewski, A. Raczynski, L. Rebarz, and J. Zaremba, Phys. Rev. A **74**, 013410 (2006).

[11] S. X. Hu and L. A. Collins, Phys. Rev. A **70**, 013407 (2004).

[12] R. Loudon, Am. J. Phys. **27**, 649 (1959).

[13] D. Xianxi, J. Dai, and J. Dai, Phys. Rev. A **55**, 2617 (1997).

[14] G. Palma and U. Raff, Can. J. Phys. **84**, 787 (2006).

[15] H. R. Reiss, Phys. Rev. A **63**, 013409 (2000).

[16] Q. Su and J. H. Eberly, Phys. Rev. A **44**, 5997 (1991).

[17] M. A. Cirone, K. Rzazewski, W. P. Schleich, F. Straub, and J. A. Wheeler, Phys. Rev. A **65**, 022101 (2001).

[18] X. L. Yang, S. H. Guo, F. T. Chan, K. W. Wong, and W. Y. Ching, Phys. Rev. A **43**, 1186 (1991).

[19] T. Dziubak and J. Matulewski, Comput. Phys. Commun. **177**, 676 (2007); A. Stathopoulos and Ch. F. Fischer, *ibid.* **79**, 268 (1994).

[20] We used the ARPACK++ package available at http://www.caam.rice.edu/software/ARPACK/; W. E. Arnoldi, Q. J. Mech. Appl. Math. **9**, 17 (1951); D. C. Sorensen, SIAM J. Matrix Anal. Appl. **13**, 357 (1992).

[21] J. Kobus, L. Laaksonen, and D. Sundholm, Comput. Phys. Commun. **98**, 346 (1996).

[22] W. H. Press, S. A. Teukolsky, W. T. Vetterling, and B. P. Flannery, *Numerical Recipes in C++*, 2nd ed. (Cambridge University Press, Cambridge, 2002).

[23] S. Geltman, J. Phys. B **33**, 1967 (2000).

[24] J. P. Hansen, J. Lu, L. B. Madsen, and H. M. Nilsen, Phys. Rev. A **64**, 033418 (2001); J. P. Hansen, T. Sørevik, and L. B. Madsen, *ibid.* **68**, 031401(R) (2003); J. Birkeland, M. Førre, J. P. Hansen, and S. Selstø, J. Phys. B **37**, 4205 (2004).

[25] L.-Y. Peng and A. F. Starace, J. Chem. Phys. **125**, 154311 (2006).

[26] http://www.phys.uni.torun.pl/~jacek/dat/